

BLACK HOLE MERGERS IN GALACTIC NUCLEI INDUCED BY THE ECCENTRIC KOZAI-LIDOV EFFECT

BAO-MINH HOANG¹, SMADAR NAOZ^{1,2}

BENCE KOCSIS³, FREDERIC A. RASIO⁴ AND FANI DOSOPOULOU⁴

¹Department of Physics and Astronomy, University of California, Los Angeles, CA 90095, USA

²Mani L. Bhaumik Institute for Theoretical Physics, Department of Physics and Astronomy, UCLA, Los Angeles, CA 90095

³Institute of Physics, Eötvös University, Pázmány P. s. 1/A, Budapest, 1117, Hungary and

⁴Center for Interdisciplinary Exploration and Research in Astrophysics (CIERA), Northwestern University, Evanston, IL 60201, USA
Draft version June 13, 2022

ABSTRACT

Nuclear star clusters around massive black holes are expected to be abundant in stellar mass black holes and black hole binaries. These binaries form a hierarchical triple system with the massive black hole at the center. Gravitational perturbations from the massive black hole can cause high eccentricity excitation. During this process, the eccentricity may approach unity, and the pericenter distance may become sufficiently small that gravitational wave emission drives the binary to merge. In this paper, we consider a simple proof of concept and explore the effect of the eccentric Kozai-Lidov mechanism for unequal mass binaries. We perform a set of Monte Carlo simulations on BH-BH binaries in galactic nuclei with quadrupole and octupole-level secular perturbations, general relativistic precession, and gravitational wave emission. For a nominal number of steady-state BH-BH binaries, our model gives a total merger rate $\sim 1-3 \text{ Gpc}^{-3} \text{ yr}^{-1}$, depending on the assumed density profile. Thus, our model potentially competes with other dynamical mechanisms, such as the dynamical formations and mergers of BH binaries in globular clusters or dense nuclear clusters without a massive black hole. We provide predictions for the distributions of these LIGO sources in galactic nuclei.

Keywords: gravitational waves – stars: kinematics and dynamics – galaxies: star clusters: general – black hole physics

1. INTRODUCTION

Recently, the Advanced Laser Interferometer Gravitational-Wave Observatory¹ (LIGO) has directly detected gravitational waves (GWs) from at least three or four inspiraling black hole-black hole (BH-BH) binaries in the Universe (LIGO Scientific and Virgo Collaboration 2016a,b, 2017). With ongoing further improvements to LIGO and the commissioning of additional instruments VIRGO² and KAGRA³, hundreds of BH-BH binary sources may be detected within the decade, opening the era of gravitational wave astronomy (The LIGO Scientific Collaboration et al. 2016).

The primary astrophysical origin of BH-BH mergers is still under debate. Merging BH binaries may be produced dynamically in dense star clusters such as globular clusters or nuclear star clusters at the center of galaxies (Portegies Zwart & McMillan 2000; Wen 2003; O’Leary et al. 2006; Antonini et al. 2014; Rodriguez et al. 2016b; O’Leary et al. 2016, 2009; Kocsis & Levin 2012; Bartos et al. 2016; Stone et al. 2016). These merging BH binaries may also be a result of isolated binary evolution in the galactic field due to special modes of stellar evolution and evolution in active galactic nuclei (Mandel & de Mink 2016; de Mink & Mandel 2016; Belczynski et al. 2016a; Marchant et al. 2016). Some studies also suggested that these LIGO detections are sourced in the first stars (Kinugawa et al. 2014, 2016; Hartwig et al. 2016; Inayoshi et al. 2016; Dvorkin et al. 2016), cores of massive stars (Reiswig et al. 2013; Loeb 2016; Woosley 2016), or dark matter halos comprised of primordial black holes (Bird et al. 2016; Clesse & García-Bellido 2016; Sasaki et al. 2016).

Here we focus on sources produced in galactic nuclei

around massive black holes (MBHs). The large escape speed in nuclear star clusters (NSCs) creates an ideal environment to accumulate a population of stellar-mass BHs. Thus, even stellar-mass BH binaries can survive in this configuration despite of supernova kicks (Lu & Naoz, in prep.). Antonini & Rasio (2016) investigated the evolution of binaries in NSCs *without MBHs in their centers*, and found a rate of $1.5 \text{ Gpc}^{-3} \text{ yr}^{-1}$. Furthermore, O’Leary et al. (2009) considered binaries that form due to gravitational wave emission during close encounters between single BHs (see also Kocsis & Levin 2012). The merger rates are dominated by massive BHs over $25 M_{\odot}$, which are delivered to the center by dynamical friction and relax to form steep density cusps near the MBH.⁴

We investigate the secular evolution of stellar-mass BH binaries in galactic nuclei *which include an MBH in their centers*. These BH-BH binaries undergo large amplitude eccentricity oscillations due to the Eccentric Kozai-Lidov (EKL, e.g., Naoz 2016) mechanism in the presence of the MBH (e.g., Antonini et al. 2010; Antonini & Perets 2012; O’Leary et al. 2009; Kocsis & Levin 2012). If the eccentricity reaches a sufficiently high value, GW emission drives the binary to merge. Recently VanLandingham et al. (2016) studied the merger rate of BH-BH binaries in the presence of intermediate massive black holes $\sim 10^{3-4} M_{\odot}$ and found it to be very efficient. Here we focus on MBHs in NSCs which are prevalent in the Universe. Antonini & Perets (2012) estimated the merger rates, in the Galactic Center, to be $1.7-4.8 \times 10^{-4} \text{ Myr}^{-1}$ from this mechanism. This rate estimation was based on the semi-analytical timescale given in Thompson (2011) and was limited to the quadrupole order in a multipole expansion. Furthermore, Antonini & Perets (2012) assumed that the heavi-

¹ <http://www.ligo.org/>

² <http://www.virgo-gw.eu/>

³ <http://gwcenter.icrr.u-tokyo.ac.jp/en/>

⁴ Mergers of low mass BHs, and neutron stars may be rare in this channel (Tsang 2013).

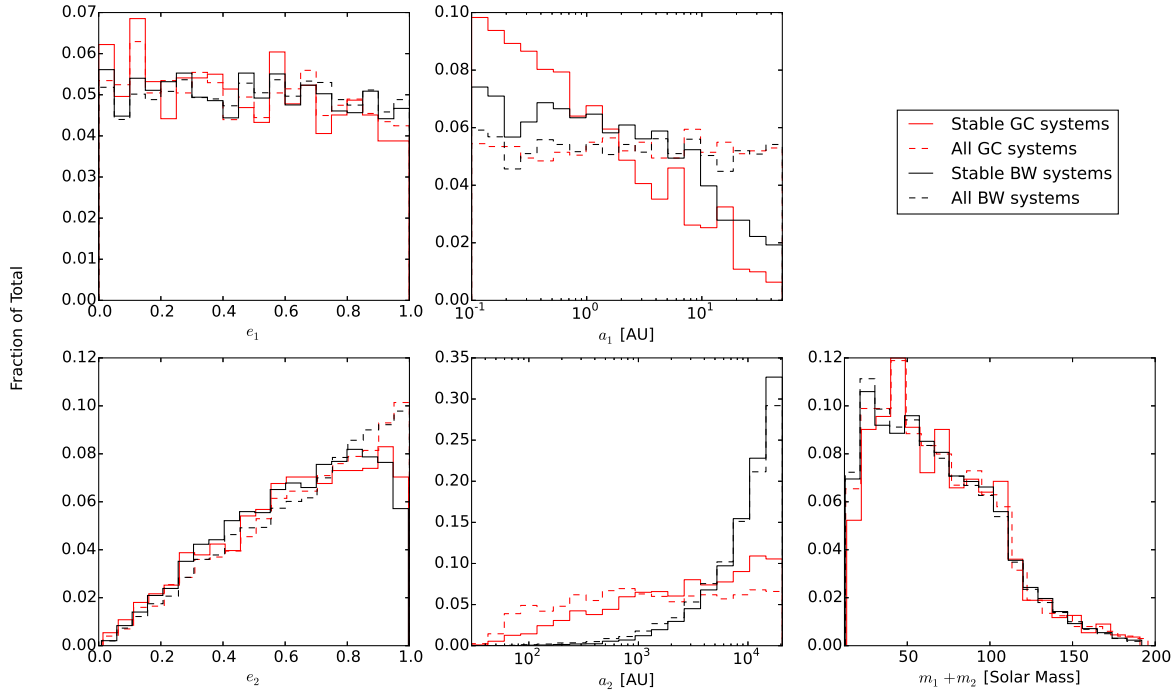


Figure 1. The initial conditions distributions before (dashed lines) and after (solid lines) accounting for stability. We consider the two density profiles we adopt, GC (red lines) and BW (black lines). The top and bottom rows depict the distribution of the inner and outer binaries, respectively, showing e, a from left to right, the bottom right panel shows the initial distribution of the total inner binary mass, $m_1 + m_2$. The mutual inclination is isotropic (uniform in $\cos i$), and the arguments of periaapsis ω_1, ω_2 are uniform from 0 to 2π . These distributions did not change after applying the stability criterion and thus are not depicted here to avoid clutter.

est BH mass in the cluster is $10M_{\odot}$.⁵ Here we use the EKL mechanism which represents the secular approximation up to the octupole level of approximation. Furthermore, we adopt a BH population consistent with a BH mass function that extends to higher masses (O’Leary et al. 2009; Kocsis & Levin 2012).

The octupole correction drives chaotic variations in the eccentricity, increases the probability of close encounters, and thus enhances the efficiency of BH-BH mergers. We show that this mechanism results in a merger rate which is higher than the rates found in the case without MBH, and it is coincidentally comparable to estimated globular cluster rates.

We describe our simulations in Section 2, and present our results, predictions and merger rate in Section 3. Finally, we offer our discussions in Section 4.

2. NUMERICAL SETUP

We study the secular dynamical evolution of binary BHs around the MBH at the center of the galaxy up to the octupole-level of approximation (e.g., Naoz 2016), including general relativity precession of the inner and outer orbits (e.g., Naoz et al. 2013), and gravitational wave emission (Peters 1964). We consider this as a simple proof of concept to investigate the effects of the EKL mechanism.

The number of BHs, their mass distribution, and number density are poorly known in NSCs. Theoretically, a single-mass distribution of objects forms a power law density cusp

⁵ The range in the rate estimation of Antonini & Perets (2012) represents core to mass-segregated distributions of the binaries, and corresponds to $\sim 0.002\text{--}0.48\text{ Gpc}^{-3}\text{ yr}^{-1}$.

around a massive object with $n(r) \propto r^{-1.75}$ (Bahcall & Wolf 1976), where $n(r)$ is the number density and r is the distance from the MBH. For multi-mass distributions, lighter and heavier objects develop shallower ($\propto r^{-1.5}$) and steeper cusps (typically $\propto r^{-2}$ to $r^{-2.2}$, and r^{-3} in extreme cases), respectively (Bahcall & Wolf 1977; Hopman & Alexander 2006b; Freitag et al. 2006; Keshet et al. 2009). Recent observations of the stellar distribution in the Milky Way NSC identify a cusp with $n(r) \propto r^{-1.25}$ (Gallego-Cano et al. 2017; Schödel et al. 2017) consistent with the profile after a Hubble time (Baumgardt et al. 2017). As BHs are heavier than typical stars, they are expected to relax into the steeper cusps. The relaxation time of BH populations is much shorter: 0.1–1 Gyr (O’Leary et al. 2009), although it can become much longer than that in the case of a shallow stellar density profile (Dosopoulou & Antonini 2017). In this paper, we assume that the BH number density follows a cusp with either $n(r) \propto r^{-2}$ or r^{-3} in our two sets of calculations. The BH mass in the two cases is set arbitrarily to 10^7 and $4 \times 10^6 M_{\odot}$, respectively, and we refer to the two models as “Bahcall-Wolf-like” (BW) and “Galactic Center” (GC) examples. Note that here “Galactic Center” refers to the assumed MBH mass (Ghez et al. 2008) and the observed stellar distribution (see below).

Note that $dN = 4\pi r^2 n(r) dr = 4\pi r^3 n(r) d(\ln r)$, where N is the number of objects, and thus we choose to have the initial outer binary semi-major axis follow a uniform distribution in a_2 and $\ln a_2$ in the BW and GC model, respectively. We set the minimum a_2 to be one at which the relaxation timescale equals the outer binary gravitational wave merger timescale. The maximum a_2 is chosen to be 0.1 pc, which corresponds

to the value at which the eccentric Kozai-Lidov timescale is equal to the timescale on which accumulated fly-bys from single stars tend to unbind the binary (see Eq. 3 and 5). However, the BH-binary semi-major axis distribution changes after applying the stability criteria (see below).

Motivated by the recent LIGO detections, in both examples the mass of each of the BHs is chosen from a distribution uniform in logspace between $6 - 100 M_\odot$ (i.e. $dN/dm \propto m^{-1}$, Miller 2002; Will 2004). The mass of the inner binary does not affect the major results from the EKL mechanism. However, it can affect the rate at which binaries become unbound due to interactions with single stars (see below). The binary separation a_1 is drawn from a uniform in log distribution between $0.1 - 50$ AU. This is consistent with Sana et al. (2012) distribution which favors short period binaries, although those BHs have already gone through stellar evolution and thus their exact distribution is unknown. We note that our stability criteria largely modifies the chosen distribution and yields a steeper distribution with a cut-off for systems beyond 50 AU, as shown in Figure 1 (see below). The lower limit is such as to avoid mass-transfer before the supernova took place. We note that the vast majority of our binaries are soft, with only 2% (5%) of the GC (BW) binaries being hard binaries (e.g., Quinlan 1996).

The eccentricity of the BH binaries is chosen from a uniform distribution (Raghavan et al. 2010) and taking the outer eccentricity distribution to be thermal (Jeans 1919). Furthermore, the inner and outer argument of periapsis ω_1 and ω_2 are chosen from a uniform distribution between 0 to 2π . In addition, the mutual inclination i is drawn from an isotropic distribution (uniform in $\cos i$).

After drawing these initial conditions we require that the systems satisfy dynamical stability, such that the hierarchical secular treatment is justified. We use two stability criteria. First we set

$$\epsilon = \frac{a_1}{a_2} \frac{e_2}{1 - e_2^2} < 0.1, \quad (1)$$

which is a measure of the relative strengths of the octupole and quadrupole level of approximations (Naoz 2016). Secondly, we require that the inner binary does not cross the Roche limit of the central MBH:

$$\frac{a_2}{a_1} > \left(\frac{3m_{MBH}}{m_{binary}} \right)^{1/3} \frac{1 + e_1}{1 - e_2}, \quad (2)$$

(e.g., Naoz & Silk 2014). These stability criteria may significantly alter the distribution of BH binary systems that can survive to long timescales around the MBH (similar to Stephan et al. 2016). We show the before and after-stability distributions in Figure 1 for both examples. We use these distributions to initialize our runs. We note that the distribution of the angles (ω_1, Ω_2 and i) remained the same after applying the stability criteria.

The main difference between the BW and GC models is the stable outer binary semi-major axis (a_2) distribution. As depicted in Figure 1, after the stability criteria $\sim 80\%$ of the BW systems remained stable, and their orbital parameter distribution did not significantly change. On the other hand, the choice of uniform in $\log(a_2)$ initial distribution for the GC case results in a steeper distribution than the nominal Bahcall & Wolf (1976) density profile, with $\sim 57\%$ of the systems remaining stable. Coincidentally, this type of steeper distribution is consistent with the de-projected density profile of the disk of massive stars (Bartko et al. 2009; Lu et al. 2009).

Moreover, this distribution represents a strongly mass segregated cluster (Keshet et al. 2009).

Gravitational perturbations from the MBH can lead to eccentricity excitation of the binary BH which may lead to mergers, via the eccentric Kozai-Lidov (EKL) mechanism (see for review Naoz 2016). We integrate the EKL equations (e.g., Naoz 2016) including GR precession and GW emission for 1000 (1500) systems in the GC (BW) case either until they merge or until they become unbound. The latter takes place on the order of the typical timescale at which close encounters with other stars in the cluster cause the binary to unbind, (e.g., Binney & Tremaine 1987). This evaporation timescale has the form:

$$t_{ev} = \frac{\sqrt{3}\sigma}{32\sqrt{\pi}G\rho a_1 \ln \Lambda} \frac{m_1 + m_2}{m_3}, \quad (3)$$

where in the inner parts ($\leq 0.1 pc$)

$$\rho = \begin{cases} 1.35 \times 10^6 M_\odot pc^{-3} (a_2/0.25 pc)^{-1.3} & \text{GC} \\ \frac{3-\alpha}{2\pi} \frac{M_{MBH}}{r^3} (G\sqrt{M_{MBH}M_0}/(\sigma_0^2 r))^{-3+\alpha} & \alpha = 1.5 \text{ BW} \end{cases} \quad (4)$$

(see, Genzel et al. 2010; Tremaine et al. 2002, for the two cases) is the density of the surrounding stars, m_1 and m_2 are the masses of the two stellar mass BHs, m_3 is the average mass of the background stars, G is the universal gravitational constant, $\ln \Lambda$ is the Coulomb logarithm, and σ is the velocity dispersion. We adopted $\ln \Lambda = 15$, $\sigma = 280 \text{ km s}^{-1} \sqrt{0.1 pc/a_2}$, and $m_3 = 1 M_\odot$ (Kocsis & Tremaine 2011). For the BW case, $\sigma_0 = 200 \text{ km s}^{-1}$ and $M_0 = 3 \times 10^8 M_\odot$ are constants. Note that the density distributions of the background stars are flatter than the density distribution of the BHs.

In the GC case, the average evaporation timescale is about 200 Myr, but there is a very broad distribution from ~ 1 Myr to ~ 3 Gyr. In the BW case, the average evaporation timescale is about 120 Myr, but again there is a broad distribution from ~ 1 Myr to ~ 2 Gyr. Binaries that do not merge are all evaporated by 10 Gyr, consistent with Stephan et al. (2016). Equation (3) linearly depends on the mass of the binary. Similar to GW150914 and GW170104, the average binary mass in the simulations is $\sim 70 M_\odot$ (see Figure 1) (LIGO Scientific and Virgo Collaboration 2016b, 2017). Adopting $10 M_\odot$ for each of the BH in the binary, as is often assumed in the literature, will increase the unbinding timescale by a factor of ~ 3.5 . As we show below, the merger timescale due to the EKL mechanism is much smaller than that. Thus, we do not expect that the binary mass will play a significant role in altering the results presented here.

3. RESULTS: EKL-INDUCED MERGERS AND GW-ONLY MERGERS

3.1. Merging Channels

The EKL mechanism has been shown to play an important role in producing short period binaries and merged systems (e.g., Thompson 2011; Naoz et al. 2011; Antonini & Perets 2012; Prodan et al. 2013; Naoz & Fabrycky 2014; Antonini & Rasio 2016; Stephan et al. 2016; Naoz et al. 2016; Naoz 2016). The high eccentricity values achieved during the binary evolution leads to a shorter GW emission timescale, which may cause a merger before the binary become unbound as shown in Figure 2. If a merger takes place due to high eccentricity excitation we denote this merger as an **EKL-induced merger**.

The eccentricity excitation due to EKL can be inhibited by GR precession if the timescale for the latter is much shorter

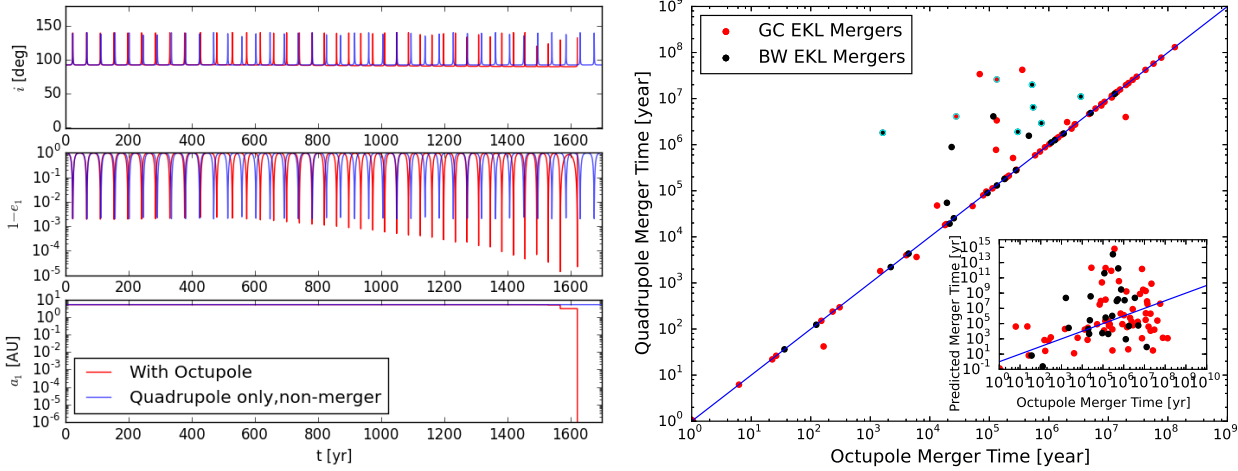


Figure 2. *Left panel:* Time evolution of the inner binary using up to the octupole level of approximation (red) and only up to the quadrupole level of approximation (blue). The initial conditions are $m_1 = 12.8 M_\odot$, $m_2 = 63.3 M_\odot$, $m_{MBH} = 1 \times 10^7 M_\odot$, $a_1 = 5.1$ AU, $a_2 = 936$ AU, $e_1 = 0.014$, $e_2 = 0.4$, $i = 92.8^\circ$. The octupole-level run results in a merger at 1623 years whereas the quadrupole-level run results in a non-merger. *Right panel:* The merger time at the quadrupole level versus the merger time at the octupole level for the EKL-induced mergers. For 16% of the GC systems and 40% of the BW systems the octupole level of approximation is important in predicting the correct merger time. For 2 of the GC systems and 6 of the BW systems, using only the quadrupole level of approximation results in a non-merger. These systems are shown with a cyan outline and the timescale shown on the y-axis is t_{ev} , (see Eq. 3). The inset shows the semi-analytical merger timescale from Thompson (2011) plotted against the merger time in the Monte-Carlo simulations.

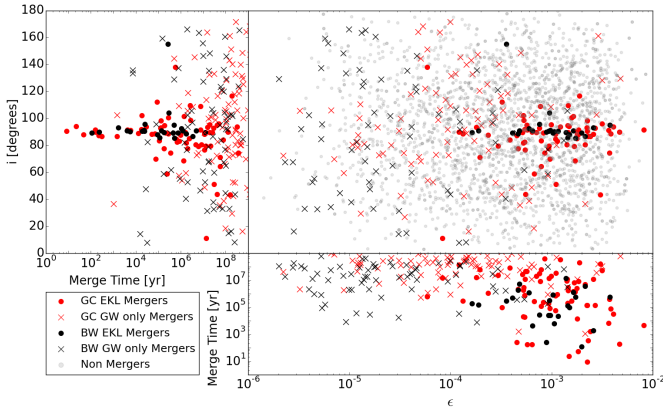


Figure 3. *Main panel:* The mutual inclination, i - ϵ plane, where ϵ is the hierarchy parameter (Eq. 1). We consider EKL mergers (red points), GW-only mergers (blue points), and non-mergers (gray points). *Left panel:* Distribution of EKL-induced and GW-only mergers for mutual inclination versus merger time. *Bottom panel:* Distribution of EKL-induced mergers and GW-only mergers for merger time versus ϵ .

than the former (e.g., Naoz et al. 2013). The EKL timescale at the quadrupole level of approximation is estimated as:

$$t_{\text{quad}} \sim \frac{16}{30\pi} \frac{m_1 + m_2 + m_3}{m_3} \frac{P_2^2}{P_1} (1 - e_2^2)^{3/2}, \quad (5)$$

(e.g., Antognini 2015), where P denotes the orbital period and the GR precession of the inner orbit timescale is:

$$t_{\text{GR,inner}} \sim 2\pi \frac{a_1^{5/2} c^2 (1 - e_1^2)}{3G^{3/2} (m_1 + m_2)^{3/2}}, \quad (6)$$

(e.g., Naoz et al. 2013) where c is the speed of light. If $t_{\text{GR,inner}} < t_{\text{quad}}$, then EKL effects are negligible, the binary evolves due to close encounters with other stars in the cluster, and the inspiral is caused only by GW emission. The binary may approach merger if the GW timescale, t_{GW} , (Peters 1964) is shorter than the timescale it takes the binary to be-

come unbound (see Equation (3)). We identify those as **GW-only mergers**.

In other words we identify two channels for mergers. In the GW-only merger we have $t_{\text{GR}} < t_{\text{quad}}$ and $t_{\text{ev}} > t_{\text{GW}}$, and in the EKL-induced merger $t_{\text{quad}} < t_{\text{GR}}$, in which the eccentricity can be excited to near unity.

The EKL-induced high eccentricity excitations usually appear in a distinctive regime in the ϵ - i parameter space. This can be seen in Figure 3, where the EKL-induced mergers inhabit a specific regime of higher ϵ (between 10^{-4} and 10^{-2}) and relatively large inclinations⁶. The EKL-induced mergers represent $\sim 7\%$ (1.7%) of all GC (BW) Monte-Carlo systems. The systems that merge via the GW-only process (where no significant eccentricity excitations took place) occupy this parameter space uniformly. They represent about 9% (9.1%) of all the GC (BW) systems. The two sub-panels in Figure 3 show that the EKL yields a systematically shorter merger timescale. In other words, out of all systems that merged, 44% are EKL-induced mergers in the GC case and about 16% are EKL-induced mergers for the BW density profile.

As implied from Figure 3 these two merger channels can yield different predictions for the statistics of BH binary mergers. The EKL-induced mergers take place preferentially in systems that are closer to the MBH (see left panel of Figure 4), whereas the GW-only systems have no apparent trend. We note that the cut-off in GW-only mergers for $a_2 < 200$ AU takes place because systems below this value either have GR precession timescale much longer than the EKL, or unbind before the binary can merge.

The EKL-induced mergers systematically happen on shorter timescales compared to the GW-only mergers (see inset on Figure 5). On average EKL-induced mergers in the GC case take place within about 25 Myrs while GW-only mergers merge on average after 296 Myrs (see Figure 5 for the merger time histogram of the two channels). On the other hand, the

⁶ Although we note, that some EKL-induced mergers take place beyond the nominal Kozai angles, (i.e., $i < 40^\circ$ and $i > 140^\circ$), which is consistent with the near co-planar behavior (Li et al. 2014).

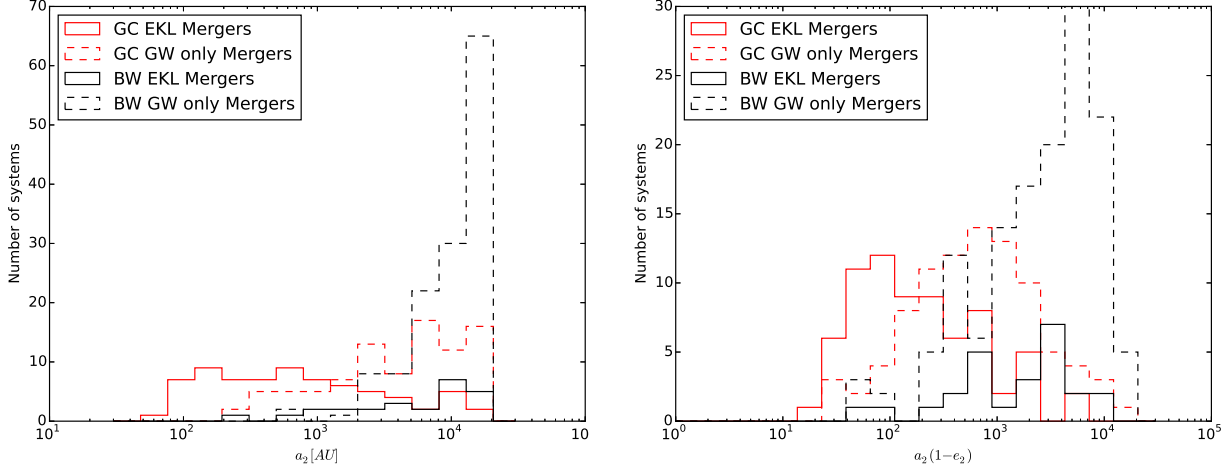


Figure 4. *Left panel* shows the histogram of a_2 . *Right panel* shows the histogram of the pericenter $a_2(1-e_2)$. We consider EKL-induced (GW-only) mergers in the BW case in solid (dashed) black lines while the GC mergers are depicted in red lines.

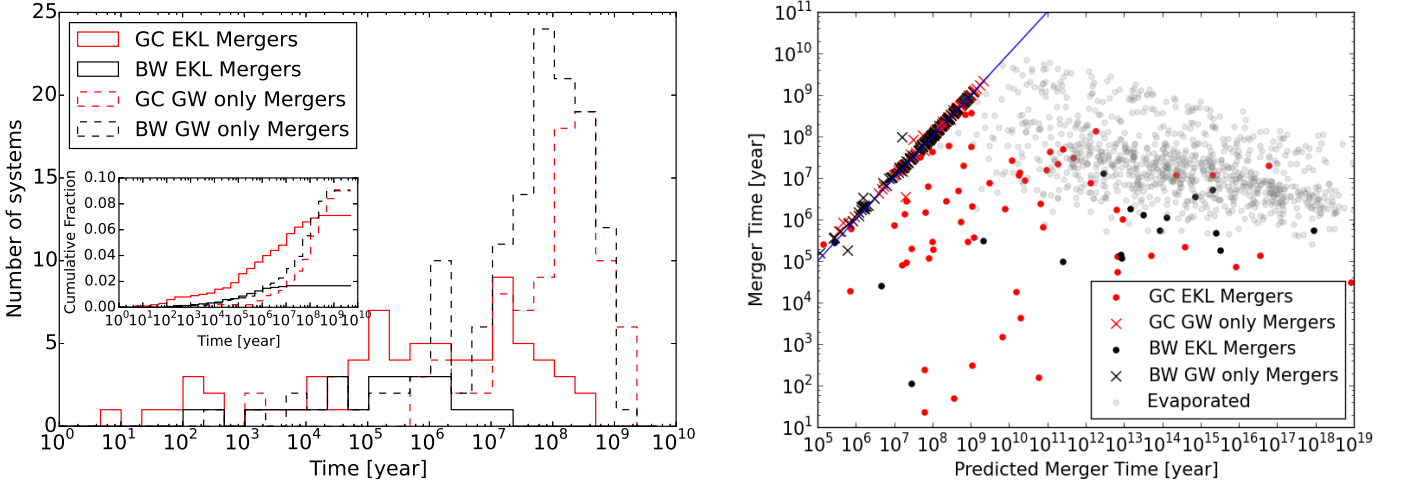


Figure 5. *GW timescale comparison between different channels.* *Left panel:* The histogram of merger times for EKL mergers (red lines) and GW-only mergers (blue lines). The *inset* shows the cumulative distribution function of merger times. *Right panel:* The actual merger timescale as a function of the GW timescale given the initial condition of the simulation. The GW-only mergers (blue points) follow the expected 1 : 1 line, while most of the EKL-induced merger times are shorter. The gray points never merge and their y-axis value marks their unbinding timescale.

BW case yields a shorter unbinding timescale and thus we get that the average EKL-induced mergers in the BW is about 1 Myr while the GW-only merger is about 166 Myr.

As expected, in both of our examples, none of the EKL-induced mergers were initially hard. On the other hand, out of the GW-only mergers, 14% in the GC example and 43% of the BW example, were, in fact, hard binaries initially. Hardening channels (e.g., [Quinlan 1996](#)) may result in a shorter merger time for those binaries.

3.2. Rate Estimate

We also estimate the merger rate of BH-BH systems. The total merger rate is dominated by the merger rate of the soft binaries because the hard binaries represent a very small percentage of the total number of systems in our simulation (2% for the GC case and 5% for the BW case). Thus, we only perform the following calculations for the soft binaries. The merger rate per unit volume is defined as:

$$\Gamma_{\text{total}} = n_g \Gamma f_{\text{MBH}}, \quad (7)$$

where n_g is the density of galaxies, Γ is the merger rate per galaxy, and f_{MBH} is the fraction of galaxies containing a MBH. We adopt $n_g = 0.02 \text{ Mpc}^{-3}$ ([Conselice et al. 2005](#)) and $f_{\text{MBH}} = 0.5$ following ([Antonini et al. 2015b,a](#)). Note that this is a rather conservative number and we expect this fraction to be higher.

The merger time for our systems ranges over large timescales with a slight systematic trend for shorter merger times closer to the MBH (i.e., smaller a_2) as can be seen in [Figure 6](#). However, these short-lived systems represent a small fraction of the total number of merged systems, and the apparent trend may be a result of statistical bias. To ascertain whether the merger rate has a dependency on a_2 , we perform a bootstrap resampling of the merger time versus the a_2 distribution. We find that the merger time distribution is roughly uniform in a_2 . Thus, the merger rate is independent of a_2 and we next consider the cumulative number of mergers as a function of time to calculate the merger rate.

[Figure 7](#) shows the cumulative number of merged systems

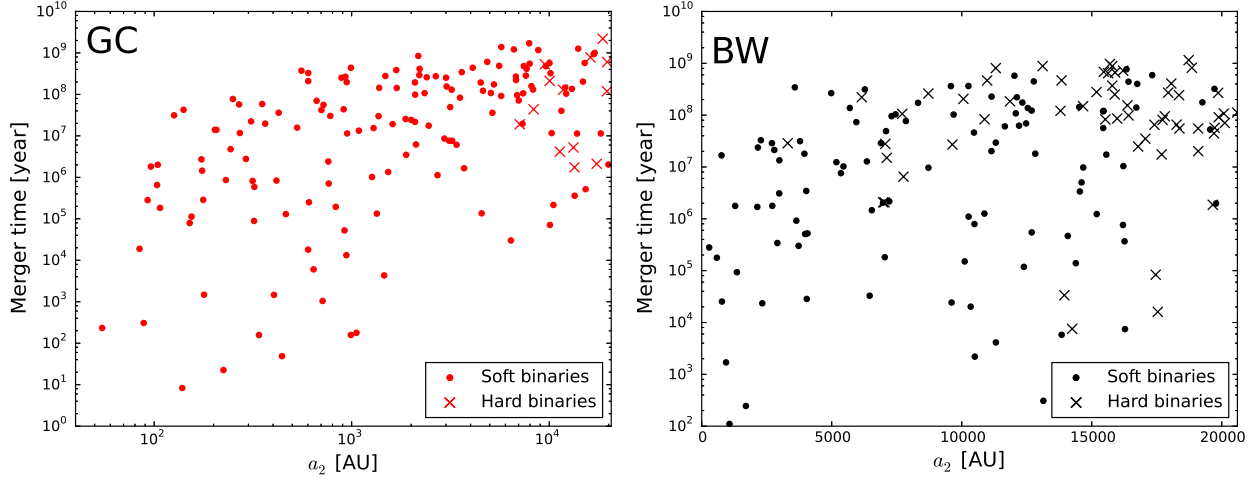


Figure 6. Merger time of soft and hard binaries as a function of outer binary separation a_2 for the GC case (left panel), and the BW case (right panel).

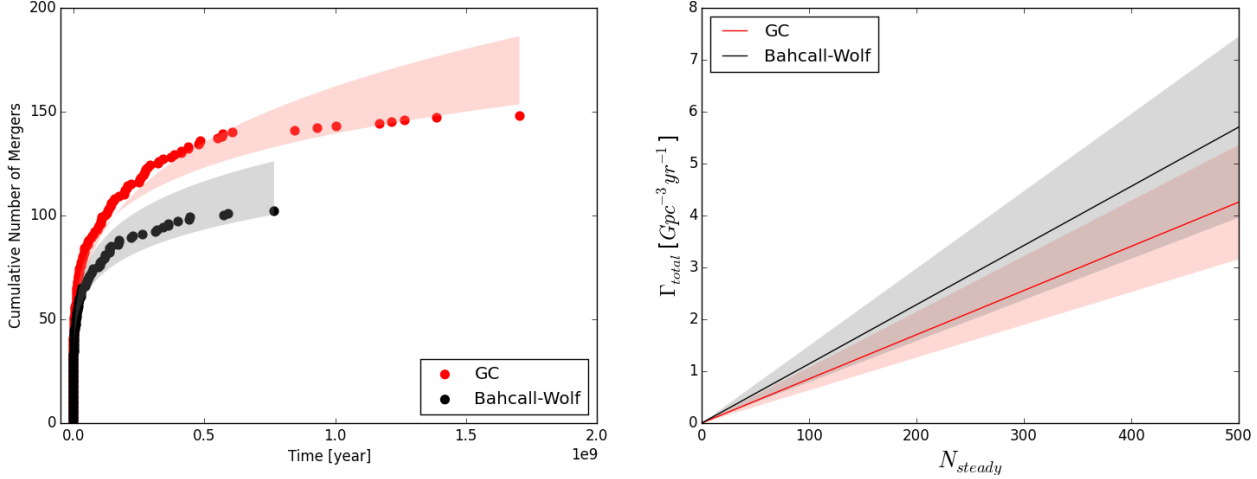


Figure 7. Left panel: Scatter points show the cumulative number of mergers as a function of time for the GC case (red) and the BW case (black). The shaded areas represent the power law fits to the 500 bootstrapped samplings. Right panel: The total merger rate Γ_{total} as a function of the number of steady state BH-BH binaries in the galactic nucleus N_{steady} . The shaded areas show upper and lower limits to the rates corresponding to the bootstrap distribution.

as a function of time. We find that it fits a power law of the form:

$$N_{merged} = a t^b, \quad (8)$$

where a and b are constants. We perform a bootstrap re-sampling on the cumulative number of mergers versus merger time distribution and generated 500 resampled data sets. We fit the above power law to all of these data sets, which gives us a range of possible fits, shown in the left panel of Figure 7. The average best fit values for a and b are 2.8 and 0.19 for the GC case, and 2.3 and 0.19 for the BW case. We note that we also fit a combination of different exponential functions to the cumulative number of mergers (not shown), which perhaps follows an exponential decay-like process. These fits were systematically less good, but nonetheless yield consistent results with those shown below. We can define a "half-life", $t_{1/2}$, for each sample as the time it takes for half of the systems that will merge to merge. Thus, the merger frequency at $t = t_{1/2}$ is:

$$\gamma = \frac{1}{N} \frac{dN}{dt} \bigg|_{t=t_{1/2}} = \frac{b}{t_{1/2}}. \quad (9)$$

We use this frequency as the characteristic merger frequency for each data set.

Assuming a steady state number of BH binaries in the galactic nucleus, N_{steady} , we can then estimate the merger rate per galaxy Γ as:

$$\Gamma = N_{steady} f_{merge} \gamma, \quad (10)$$

where f_{merge} is the merger fraction from our simulation, equal to 0.11 for the GC case and 0.07 for the BW case. N_{steady} is highly uncertain, so we set it to be a free parameter between 1 and 500. The right panel of Figure 7 shows the total merger rate as a function of N_{steady} . Hopman & Alexander (2006b) estimated the number of steady state BHs within 0.1 pc of the MBH to be 1800. Assuming that 10% of these BHs are in binaries we obtain ~ 180 binary BHs (Belczynski et al. 2016b). We use $N_{steady} = 180$ to calculate nominal merger rates for the GC and BW cases. We find a nominal average merger rate of $\sim 1.5 \text{ Gpc}^{-3} \text{ yr}^{-1}$ for the GC case and $\sim 2 \text{ Gpc}^{-3} \text{ yr}^{-1}$ for the BW case. These average merger rate values are represented by the solid lines in the right panel of Figure 7; the merger rate range obtained from the bootstrap is depicted by the shaded

areas.

Our estimated merger rates are on the same order as the merger rates estimated for globular clusters, $5 \text{ Gpc}^{-3} \text{ yr}^{-1}$ (Rodriguez et al. 2016a), isolated triples in galaxies $0.14\text{--}6 \text{ Gpc}^{-3} \text{ yr}^{-1}$ (Silsbee & Tremaine 2016), and mergers following close encounters of initially unbound BHs $0.04\text{--}3 \text{ Gpc}^{-3} \text{ yr}^{-1}$ (O’Leary et al. 2009)⁷. The current LIGO/VIRGO detection constrain the total merger rate of circular BH binaries to within $12\text{--}240 \text{ Gpc}^{-3} \text{ yr}^{-1}$ (LIGO Scientific and Virgo Collaboration 2017).

Note that Antonini & Perets (2012) rate estimation is based on the quadrupole based semi-analytical timescale which does not capture the system’s full dynamical behavior. The octupole level of approximation, used here, shortens the merger timescale for 16%–40% of the EKL-induced mergers, for the GC and BW distributions, respectively (see Figure 2). Furthermore, Antonini & Perets (2012) used the semi-analytical timescale given in Thompson (2011) to estimate the merger timescale. However, this clearly does not capture the correct merger timescale as can be deduced from the inset in Figure 2.

The estimate reported here is subject to the following caveats. First, we have neglected the mass precession of the outer binary, which occurs on a timescale of $t_{\text{prec}} \sim 4 \times 10^4 \text{ yr}$ (Kocsis & Tremaine 2011). This precession occurs on a timescale which is longer than the quadrupole timescale, although it may be comparable to the octupole timescale (e.g., Li et al. 2015). Future work is needed to determine the extent of the effect this precession has on the dynamics of the system. We have also neglected the effects of resonant relaxation, as they should be added self-consistently (Rauch & Tremaine 1996; Sridhar & Touma 2016). These effects operate on longer timescales than the quadrupole timescale. However, they can refill the high inclination EKL regime in some cases, causing further eccentricity excitation. This is beyond the scope of this paper. Recently Petrovich & Antonini (2017) showed that variations from spherical symmetry in the potential may induce eccentricity excitation at large a_2 . Thus, their proposed mechanism may even increase the merger rate discussed here for systems at larger distances. However, their study also neglected vector resonant relaxation which operates on the same timescales and distances. Therefore, further investigation is needed for a more accurate treatment of these effects.

Secondly, we have assumed a steady state distribution of BH binaries corresponding to a relaxed cluster. Relaxing the steady state assumption means that the EKL-induced mergers will be depleted quickly, as implied from Figure 5. The binary population may be replenished from the outside, for example from globular clusters or from star formation (e.g., Hopman & Alexander 2006a,b; Gnedin et al. 2014; Antonini et al. 2015a). A possible channel for the formation of new BH binaries in the center of the galaxies may lay in E+A, or poststarburst galaxies (e.g., Dressler & Gunn 1983). These galaxies are special because it appears that they underwent a star formation episode that terminated abruptly $\sim 1 \text{ Gyr}$ ago. Thus, this population may hold recent BH-BH binaries near their nuclei. While these galaxies are a relatively rare subtype of elliptical galaxies, they may increase the stellar mass of the

galaxy by $\sim 10\%$ (e.g., Swinbank et al. 2012). Thus, due to their recent star formation and overdensity in the nuclei, these galaxies were linked to an enhancement of tidal disruption events (e.g., Arcavi et al. 2014; Stone & van Velzen 2016). Therefore, these galaxies may have an overabundance of BH binaries, which can cause enhancement of BH-BH mergers.

4. DISCUSSION

We investigated the secular evolution of stellar-mass BH binaries in the neighborhood of the MBH in galactic nuclei using Monte Carlo simulations. Our equations included the hierarchical secular effects up to the octupole-level of approximation (the so-called EKL mechanism, Naoz 2016), and general relativity precession of the inner and outer orbits as well as and gravitational wave emission between the two stellar BHs. During their evolution, binary stellar mass BHs may undergo large eccentricity excitations which can drive them to merge (see for example Figure 2). While BHs are expected to segregate toward the center of the galactic nuclei, the power law index of the number density of the cusp is still uncertain. As a proof-of-concept, we explored two cases: r^{-2} , denoted as BW; and r^{-3} , denoted as GC. We find a consistent merger rate in both cases.

We identified two channels for BH-BH mergers. In the first type of merger, the general relativity precession timescale is shorter than the quadrupole timescale, suppressing eccentricity excitations. However, the initial GW merger timescale is shorter than the evaporation timescale, leading to a merger. We call these GW-only mergers. These systems will merge in the absence of an MBH in the center of a galaxy. For the second type of merger, the EKL mechanism produces large eccentricity oscillations in the inner binary orbit, driving the binary BHs to merge. We call these EKL-induced mergers.

GW-only and EKL-induced mergers occupy different parts of the parameter space for both number density profiles we examined. Specifically, considering the ϵ – i parameter space, where ϵ is given by Eq. (1). EKL-induced mergers will preferentially occupy a regime of high ϵ and close to 90° mutual inclination. On the other hand, GW-only mergers are uniformly spread in this parameter space (see Figure 3). This yields a prediction for the merger distribution as a function of distance from the MBH: the EKL-induced mergers will be systematically closer to the MBH. This is depicted in Figure 4.

Finally we estimate the total merger rate to be at the order of unity and perhaps even higher. This rate is coincidentally comparable to the estimated merger rate in globular clusters, which suggests that galactic nuclei may host a significant fraction of the BH-BH mergers. Note that Antonini & Rasio (2016) showed that if the natal kick of BH binaries is higher than 50 km sec^{-1} then the efficiency of forming BH binaries in globular clusters is suppressed significantly (Chatterjee et al. 2017)⁸, and BH mergers in nuclear star clusters dominate over mergers in globular clusters. In this case, mergers in nuclear star clusters that contain an MBH may dominate over all other types of mergers. We note that, if natal kicks are smaller, so that BH binaries form efficiently in globular clusters, BH mergers in nuclear star cluster with an MBH is still comparable to that of globular clusters.

The BH-BH merger scenario presented here, in our proof-of-concept examples, suggests that MBH gravitational per-

⁷ Here we use the rates per single galaxy in O’Leary et al. (2009) Table 1 and multiply by $\xi = 10$ and $n_g = 0.02 \text{ Mpc}^{-3}$. However, that mechanism is weakly sensitive to the NSC and MBH mass. Dwarf galaxies dominate the rates with a much higher n_g .

⁸ And also above this natal kick the mergers of isolated binaries is significantly suppressed (Belczynski et al. 2016b)

turbations can enhance the merger rate. We have provided the parameter space at which these mergers take place, and demonstrated that they occupy a different part of the parameter space. This suggests that this channel may be statistically distinguished with a sufficiently large sample of mergers (Hoang et al. in prep.).

We thank Michael Fitzgerald for insightful discussions about statistical analysis. BMH acknowledges the support of the Eugene V. Cota-Robles Fellowship and the Graduate Dean's Scholar Award. SN acknowledges partial support from a Sloan Foundation Fellowship. FAR and FD acknowledge support from NASA Grant NNX14AP92G and NSF Grant AST-1716762 at Northwestern University. This work was supported in part by the European Research Council under the European Union's Horizon 2020 Programme, ERC Starting Grant #638435 (GalNUC).

REFERENCES

- Abbott, B. P., Abbott, R., Abbott, T. D., et al. 2016a, *Physical Review X*, **6**, 041015
- . 2016b, *Physical Review Letters*, **116**, 061102
- Antognini, J. M. O. 2015, ArXiv e-prints, [arXiv:1504.05957 \[astro-ph.EP\]](#)
- Antonini, F., Barausse, E., & Silk, J. 2015a, *ApJ*, **812**, 72
- . 2015b, *ApJ*, **806**, L8
- Antonini, F., Faber, J., Gualandris, A., & Merritt, D. 2010, *ApJ*, **713**, 90
- Antonini, F., Murray, N., & Mikkola, S. 2014, *ApJ*, **781**, 45
- Antonini, F., & Perets, H. B. 2012, *ApJ*, **757**, 27
- Antonini, F., & Rasio, F. A. 2016, *ApJ*, **831**, 187
- Arcavi, I., Gal-Yam, A., Sullivan, M., et al. 2014, *ApJ*, **793**, 38
- Bahcall, J. N., & Wolf, R. A. 1976, *ApJ*, **209**, 214
- . 1977, *ApJ*, **216**, 883
- Bartko, H., Martins, F., Fritz, T. K., et al. 2009, *ApJ*, **697**, 1741
- Bartos, I., Kocsis, B., Haiman, Z., & Márka, S. 2016, ArXiv e-prints, [arXiv:1602.03831 \[astro-ph.HE\]](#)
- Baumgardt, H., Amaro-Seoane, P., & Schödel, R. 2017, ArXiv e-prints, [arXiv:1701.03818](#)
- Belczynski, K., Holz, D. E., Bulik, T., & O'Shaughnessy, R. 2016a, ArXiv e-prints, [arXiv:1602.04531 \[astro-ph.HE\]](#)
- Belczynski, K., Repetto, S., Holz, D. E., et al. 2016b, *ApJ*, **819**, 108
- Binney, J., & Tremaine, S. 1987, *Galactic dynamics*
- Bird, S., Cholis, I., Muñoz, J. B., et al. 2016, ArXiv e-prints, [arXiv:1603.00464](#)
- Chang, P. 2009, *MNRAS*, **393**, 224
- Chatterjee, S., Rodriguez, C. L., & Rasio, F. A. 2017, *ApJ*, **834**, 68
- Clesse, S., & García-Bellido, J. 2016, ArXiv e-prints, [arXiv:1603.05234](#)
- Conselice, C. J., Blackburne, J. A., & Papovich, C. 2005, *ApJ*, **620**, 564
- de Mink, S. E., & Mandel, I. 2016, ArXiv e-prints, [arXiv:1603.02291 \[astro-ph.HE\]](#)
- Dosopoulou, F., & Antonini, F. 2017, *ApJ*, **840**, 31
- Dressler, A., & Gunn, J. E. 1983, *ApJ*, **270**, 7
- Dvorkin, I., Vangioni, E., Silk, J., Uzan, J.-P., & Olive, K. A. 2016, ArXiv e-prints, [arXiv:1604.04288 \[astro-ph.HE\]](#)
- Freitag, M., Amaro-Seoane, P., & Kalogera, V. 2006, *ApJ*, **649**, 91
- Gallego-Cano, E., Schödel, R., Dong, H., et al. 2017, ArXiv e-prints, [arXiv:1701.03816](#)
- Genzel, R., Eisenhauer, F., & Gillessen, S. 2010, *Reviews of Modern Physics*, **82**, 3121
- Ghez, A. M., Salim, S., Weinberg, N. N., et al. 2008, *ApJ*, **689**, 1044
- Gnedin, O. Y., Ostriker, J. P., & Tremaine, S. 2014, *ApJ*, **785**, 71
- Hartwig, T., Volonteri, M., Bromm, V., et al. 2016, ArXiv e-prints, [arXiv:1603.05655](#)
- Hopman, C. 2009, *ApJ*, **700**, 1933
- Hopman, C., & Alexander, T. 2006a, *ApJ*, **645**, 1152
- . 2006b, *ApJ*, **645**, L133
- Inayoshi, K., Kashiyama, K., Visbal, E., & Haiman, Z. 2016, ArXiv e-prints, [arXiv:1603.06921](#)
- Jeans, J. H. 1919, *MNRAS*, **79**, 408
- Keshet, U., Hopman, C., & Alexander, T. 2009, *ApJ*, **698**, L64
- Kinugawa, T., Inayoshi, K., Hotokezaka, K., Nakauchi, D., & Nakamura, T. 2014, *MNRAS*, **442**, 2963
- Kinugawa, T., Miyamoto, A., Kanda, N., & Nakamura, T. 2016, *MNRAS*, **456**, 1093
- Kocsis, B., & Levin, J. 2012, *Phys. Rev. D*, **85**, 123005
- Kocsis, B., & Tremaine, S. 2011, *MNRAS*, **412**, 187
- Li, G., Naoz, S., Kocsis, B., & Loeb, A. 2014, *ApJ*, **785**, 116
- . 2015, *MNRAS*, **451**, 1341
- LIGO Scientific and Virgo Collaboration. 2016a, *Phys. Rev. Lett.*, **116**, 241103
- . 2016b, *Phys. Rev. Lett.*, **116**, 061102
- . 2017, *Phys. Rev. Lett.*, **118**, 221101
- Loeb, A. 2016, *ApJ*, **819**, L21
- Lu, J. R., Ghez, A. M., Hornstein, S. D., et al. 2009, *ApJ*, **690**, 1463
- Mandel, I., & de Mink, S. E. 2016, ArXiv e-prints, [arXiv:1601.00007 \[astro-ph.HE\]](#)
- Marchant, P., Langer, N., Podsiadlowski, P., Tauris, T., & Moriya, T. 2016, ArXiv e-prints, [arXiv:1601.03718 \[astro-ph.SR\]](#)
- Miller, M. C. 2002, *ApJ*, **581**, 438
- Naoz, S. 2016, *ARA&A*, **54**, (Volume publication date September 2016)
- Naoz, S., & Fabrycky, D. C. 2014, *ApJ*, **793**, 137
- Naoz, S., Farr, W. M., Lithwick, Y., Rasio, F. A., & Teyssandier, J. 2011, *Nature*, **473**, 187
- Naoz, S., Fragos, T., Geller, A., Stephan, A. P., & Rasio, F. A. 2016, *ApJ*, **822**, L24
- Naoz, S., Kocsis, B., Loeb, A., & Yunes, N. 2013, *ApJ*, **773**, 187
- Naoz, S., & Silk, J. 2014, *ApJ*, **795**, 102
- O'Leary, R. M., Kocsis, B., & Loeb, A. 2009, *MNRAS*, **395**, 2127
- O'Leary, R. M., Meiron, Y., & Kocsis, B. 2016, ArXiv e-prints, [arXiv:1602.02809 \[astro-ph.HE\]](#)
- O'Leary, R. M., Rasio, F. A., Fregeau, J. M., Ivanova, N., & O'Shaughnessy, R. 2006, *ApJ*, **637**, 937
- Peters, P. C. 1964, *Physical Review*, **136**, 1224
- Petrovich, C., & Antonini, F. 2017, ArXiv e-prints, [arXiv:1705.05848 \[astro-ph.HE\]](#)
- Portegies Zwart, S. F., & McMillan, S. L. W. 2000, *ApJ*, **528**, L17
- Prodan, S., Murray, N., & Thompson, T. A. 2013, ArXiv e-prints, [arXiv:1305.2191 \[astro-ph.SR\]](#)
- Quinlan, G. D. 1996, *NA*, **1**, 35
- Raghavan, D., McAlister, H. A., Henry, T. J., et al. 2010, *ApJS*, **190**, 1
- Rauch, K. P., & Tremaine, S. 1996, *NewA*, **1**, 149
- Reisswig, C., Ott, C. D., Abdikamalov, E., et al. 2013, *Physical Review Letters*, **111**, 151101
- Rodriguez, C. L., Chatterjee, S., & Rasio, F. A. 2016a, *Phys. Rev. D*, **93**, 084029
- Rodriguez, C. L., Morscher, M., Wang, L., et al. 2016b, ArXiv e-prints, [arXiv:1601.04227 \[astro-ph.IM\]](#)
- Sana, H., de Mink, S. E., de Koter, A., et al. 2012, *Science*, **337**, 444
- Sasaki, M., Suyama, T., Tanaka, T., & Yokoyama, S. 2016, ArXiv e-prints, [arXiv:1603.08338](#)
- Schödel, R., Gallego-Cano, E., Dong, H., et al. 2017, ArXiv e-prints, [arXiv:1701.03817](#)
- Silber, K., & Tremaine, S. 2016, ArXiv e-prints, [arXiv:1608.07642 \[astro-ph.HE\]](#)
- Sridhar, S., & Touma, J. R. 2016, *MNRAS*, **458**, 4143
- Stephan, A. P., Naoz, S., Ghez, A. M., et al. 2016, *MNRAS*, **460**, 3494
- Stone, N. C., Metzger, B. D., & Haiman, Z. 2016, ArXiv e-prints, [arXiv:1602.04226](#)
- Stone, N. C., & van Velzen, S. 2016, *ApJ*, **825**, L14
- Swinbank, A. M., Balogh, M. L., Bower, R. G., et al. 2012, *MNRAS*, **420**, 672
- The LIGO Scientific Collaboration, & the Virgo Collaboration. 2016, ArXiv e-prints, [arXiv:1602.03839 \[gr-qc\]](#)
- The LIGO Scientific Collaboration, the Virgo Collaboration, Abbott, B. P., et al. 2016, ArXiv e-prints, [arXiv:1606.04856 \[gr-qc\]](#)
- Thompson, T. A. 2011, *ApJ*, **741**, 82
- Tremaine, S., Gebhardt, K., Bender, R., et al. 2002, *ApJ*, **574**, 740
- Tsang, D. 2013, *ApJ*, **777**, 103
- VanLandingham, J. H., Miller, M. C., Hamilton, D. P., & Richardson, D. C. 2016, *ApJ*, **828**, 77
- Wen, L. 2003, *ApJ*, **598**, 419
- Will, C. M. 2004, *ApJ*, **611**, 1080
- Woosley, S. E. 2016, ArXiv e-prints, [arXiv:1603.00511 \[astro-ph.HE\]](#)